

VISUALIZATION OF MOBILE MAPPING DATA VIA PARALLAX SCROLLING

D. Eggert^a, E. C. Schulze^b

Institute of Cartography and Geoinformatics, Leibniz Universität Hannover, Germany -
^a eggert@ikg.uni-hannover.de, ^b mmboxbox@googlemail.com

Commission III, WG III/5

KEY WORDS: Point-cloud, Visualization, Mobile Mapping, Parallax Scrolling, Image-based rendering, Real-time rendering

ABSTRACT:

Visualizing big point-clouds, such as those derived from mobile mapping data, is not an easy task. Therefore many approaches have been proposed, based on either reducing the overall amount of data or the amount of data that is currently displayed to the user. Furthermore, an entirely free navigation within such a point-cloud is also not always intuitive using the usual input devices. This work proposes a visualization scheme for massive mobile mapping data inspired by a multiplane camera model also known as parallax scrolling. This technique, albeit entirely two-dimensional, creates a depth illusion by moving a number of overlapping partially transparent image layers at various speeds. The generation of such layered models from mobile mapping data greatly reduces the amount of data up to about 98% depending on the used image resolution. Finally, it is well suited for the panoramic-fashioned visualization of the environment of a moving car.

1. INTRODUCTION

The visualization of large amounts of data usually yields various problems. Either the user is overwhelmed by the sheer volume of information and therefore maybe missing the features important to him or the hardware displaying the data reaches its limit and is unable to provide interactive framerates. One way to face these problems is to reduce the amount of data (or generalize it) to such an extent that the above constraints are met.

One way of generalization is dimensionality-reduction. In case of mobile mapping we have to deal with colored three dimensional point-clouds. Reducing the data about the height property for example, results in map-like representation as shown in figure 1.

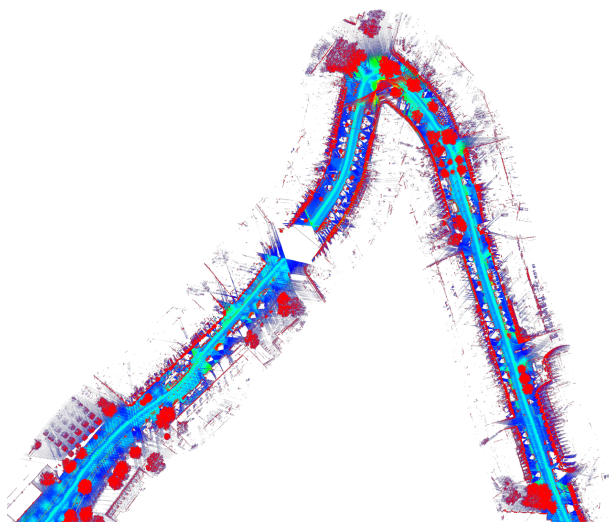


Figure 1: 2D map derived from mobile mapping point-cloud by eliminating the height property.

While this kind of visualization gives a nice overview of the scene it also eliminates all uprising structures like facades. In order keep the facade structures the height property has to be kept as

well. An alternative property to reduce would be the depth property. Since this property depends on the point of view (POV), eliminating the depth results in a limitation of possible POVs. This fact raises two questions, first which POVs shall be used and second how does it impact the navigation through the data.

Since the visualization aims for displaying mobile mapping, it felt natural using the acquisition vehicle's track as possible POVs. Restricting the virtual camera to those POVs enables the visualization to handle areas of missing information in a sophisticated manner as discussed in chapter 5. The impact on the navigation is noticeable. The scene can only be seen from the given trajectory points, so the only real navigation option the user has is to move forward or backward on the trajectory. Furthermore the viewing direction is also fixed, which means only one street-side can be watched at a time. While this appears to be a significant limitation it simplifies the navigation through the rather complex data as well. This simple navigation enables even non experienced users to easily browse through the mobile mapping data. Which makes the proposed visualization scheme more comparable to systems like Google's Streetview (Vincent, 2007) and Microsoft's Street-slide (Kopf et al., 2010) as to systems visualizing a complete 3D city model.

Finally, in order to regain at least a sense or an illusion of depth the concept of parallax scrolling comes into play. Instead of entirely eliminating the depth property it is only clustered into discrete values, resulting in various depth layers. Rendering those layers on top of each other, as shown in figure 2 gives an illusion of depth which improves the quality of visualization compared to an entirely flat one, as shown in figure 1.



Figure 2: Resulting parallax scrolling visualization with color-labeled depth layers.

2. RELATED WORK

Over the years the processing and visualization of large point-clouds have been addressed by various publications.

In general most approaches can be classified into two categories. First the point-clouds can be generalized into simpler models with a lower level of detail (LOD). This reduces the amount of data significantly, but might remove relevant features from the data. One example from this category was published by (Wahl et al., 2005), where planes within a point-cloud are identified and points belonging to those planes are projected onto texture representations. This is based on the idea of exchanging geometry information with texture information which increases the rendering speed. This is also often referred to as image-based representations for reducing the geometric complexity. (Jeschke et al., 2005) gives good overview of such approaches. In contrast to purely point based data in case of mobile mapping, impostors based methods like in (Wimmer et al., 2001) usually use 3D mesh models as their input data. The creation of such meshes are out of the scope of this work and thus using impostors is not a viable option, while the general idea will be applied in the presented work.

The second category simply reduces the data, in case of point-clouds the number of points, that is displayed at a time, e.g. by skipping points or regions that are currently not visible on screen. In case the points become visible they are loaded into memory, while the points and regions becoming invisible are dropped from the memory. Those approaches are usually referred to as out-of-core methods. In the end methods fusing both approaches (generalized models and out-of-core techniques) do also exist, rendering far away objects with a low LOD, while increasing the LOD in case the objects are getting closer. (Richter and Döllner, 2010) and (Gobetti and Marton, 2004) discuss two varieties of such approaches.

Since this work uses the concept of parallax scrolling which is based on image-based rendering, it belongs to the first domain of generalization of point-clouds.

Occlusions are a major problem when it comes to deriving models from point-cloud data. As the texture images are derived from the recorded scan-points, they only convey information that was observed by the corresponding laser. Objects not reflecting the laser beam (e.g. windows) as well as objects or areas, occluded by other foreground objects do not appear in the generated images. Since the images have to be transparent for the parallax scrolling rendering, the missing areas result in transparent holes. Those holes can be closed by interpolation, either in the original point-cloud like shown in (Wang and Oliveira, 2007) or in the resulting image as shown in (Efros and Leung, 1999). But as the actual origin is not entirely known, interpolation could lead to an overall wrong model. The restricted virtual camera dictated by the used visualization scheme allows to deal with those holes in different manners. Instead of filling them up they can also be hidden in more or less the same way they were hidden from the laser beam.

3. PARALLAX SCROLLING

Parallax Scrolling is a visualization method, which creates a depth illusion in an animated, two dimensional scene. For this it uses multiple layers of two dimensional graphics, which are displayed on top of each other, thus forming a single image for the camera, which looks down at the top of the stack. In order to simulate a camera movement, each layer is moved at its own speed, instead

of moving the camera it self. Figure 3 elucidates this by showing a series of three pictures with layers moving at different speeds.

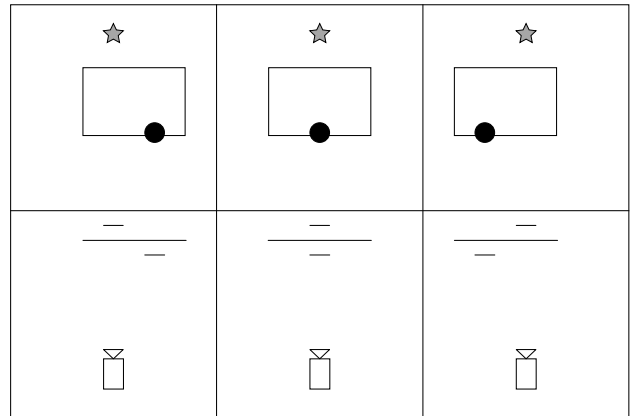


Figure 3: Sketch of parallax scrolling scene with simulated camera movement from left to right. Upper row: The images that the camera sees. Lower row: The camera looking at the layers.

3.1 Mathematics Behind Parallax Scrolling

For a general visualization with parallax scrolling one needs a sequence L of layers l_i . Let $L = \langle l_1, l_2, \dots, l_n \rangle$ be ordered such that l_1 is at the top of the stack, meaning closest to the camera, and l_n is at the bottom of the stack, meaning the farthest away from the camera. Each layer i has, next to its image data, a two-dimensional position $\vec{p}_i = \begin{pmatrix} x_i \\ y_i \end{pmatrix}$ and a speed v_i , as well as *width* and *height*.

In order to display the entire scene, we must render each layer of the stack beginning at the bottom and ending at the top. This way the rendered image will only contain pixels, which are not occluded by other layers.

As mentioned before the camera is always steady, hence to virtually move the Camera by $\vec{\Delta} = \begin{pmatrix} x_{\Delta} \\ y_{\Delta} \end{pmatrix}$, we have to shift each layer's position in respect to its speed instead. The new positions \vec{p}_i' are calculated as follows:

$$\vec{p}_i' = \vec{p}_i - v_i \cdot \vec{\Delta} \quad (1)$$

3.2 Perspective Parallax Scrolling

Simply rendering various image layers on top of each other results in an orthogonal projection, which might appear quite unnatural. In order to create a more appealing perspective correct parallax scrolling, we need to calculate the layer-speeds v_i . Furthermore, we also need to calculate a scaling factor s_i for each layer, to simulate the fact that an object looks smaller the bigger the distance to the observer is.

Let α be the horizontal aperture of the camera. Also let d_i be the distance of the i -th layer to the camera. Now we calculate the distance r at which one length unit in the model matches one length unit in the image (see figure 4).

$$r = \frac{1}{2} \cdot \cot\left(\frac{\alpha}{2}\right) \quad (2)$$

It follows that objects at half that distance appear twice as big in both dimensions, while objects at double that distance appear

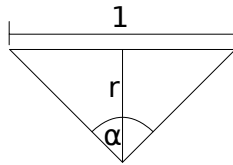


Figure 4: Sketch of the calculation of r .

half as big in both dimensions. Therefore the scaling factor s_i is calculated as follows:

$$s_i = \frac{r}{d_i} \quad (3)$$

The same argument can be used to calculate the speed v_i , which means that $v_i = s_i$.

In order to finally draw the scene the new corner positions for each layer have to be calculated. Let \vec{p} be a corner position of the i -th layer. Also, let \vec{c} be the camera position and z be the camera zoom factor. The new position of the corner is calculated as follows:

$$\vec{p}' = z \cdot (s_i \cdot \vec{p} - v_i \cdot \vec{c}) = z \cdot s_i \cdot (\vec{p} - \vec{c}) \quad (4)$$

With the known corners the layer image can be scaled and drawn accordingly.

4. MODEL GENERATION

Visualizing the mobile mapping data using the parallax scrolling technique requires the data to be ordered in layers. Each layer represents a distinct depth or depth-range. Considering mobile mapping relevant layers can be (in ascending distance from the acquisition vehicle) cars (on the road), parking cars, street furniture (traffic signs, traffic lights, trees, etc.), pedestrians and finally the building facades.

4.1 Identification of relevant layers

In order to identify those relevant layers mentioned above many approaches are feasible. This paper discusses two approaches (geometry-based and semantic-based).

The first method is purely based on the geometry of the point-cloud input data. First of all the acquisition vehicle's track is simplified, while the resulting track segments are used to find relevant layers. To this end a buffer around each segment is defined and two histograms (one for each street-side) reflecting the distances of all scan-points within this buffer towards the corresponding track segment are created. Figure 5 shows a typical distance histogram.

While the maximum peak usually represents the building facade layer, all minor peaks represent object layers. In order to extract the position and size of each layer the current maximum peak is used as the start value, while all neighboring distances, to the left as well as to the right, will be assigned to this maximum peak until a value below a given threshold is found and a minimum number of points had been assigned. After removing all assigned values from the histogram the process recursively identifies the remaining layers by again starting at the maximum peak value. Since the building facade layer is likely to be the most distant relevant layer all values behind the first maximum peak are assigned

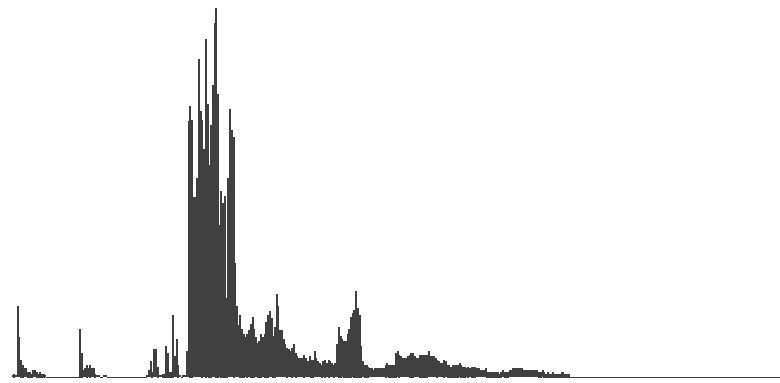


Figure 5: Distance histogram of all points on a single street-side for a given track segment.

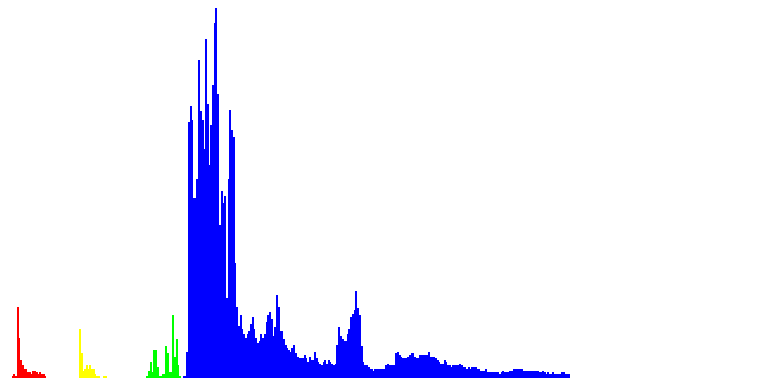


Figure 6: Distance histogram with color-encoded relevant layers.

to this layer. Figure 6 shows a possible result, with all identified relevant layers.

The second, semantic-based approach is based on segmenting and classifying the point-cloud. Our segmentation method first extracts all ground points from the point-cloud using a normal-based region-growing. This leaves all remaining objects unconnected, hence all objects are again segmented by region-growing. Depending on the desired visualization scenario the all segmented objects have to be classified. Within the scope of this work we merely classified the objects into *building/facade* and *other*. Finally the relevant building layer is derived from the classified building objects by detecting the major facade plane using the RANSAC, see (Fischler and Bolles, 1981), plane-fit method. All remaining objects are represented by a track-segment parallel layer passing through the object's center of mass.

4.2 Final Layer-Model

After the relevant layers have been detected the corresponding texture representation is generated by projecting the associated points onto the respective layer planes. Depending on the point-cloud's density and the used image-resolution the resulting image can appear quite sparse. In order to face this intermediate pixels can be interpolated accordingly. Both the point to plane projection as well as the pixel interpolation are in detail covered by (Eggert and Sester, 2013). An exemplary image is shown in figure 7.

The result is a layer-model consisting of multiple translucent texture images which will eventually rendered by the parallax scrolling visualization.



Figure 7: Resulting texture image representing a single layer

5. HIDING BLIND SPOTS AND HOLE-FILLING

During the mobile mapping process it will often be the case, that some objects are partially occluded by others, e.g. a parking car in front of a house. Since the LiDAR's laser beams do generally not pass through solid objects, this leads to volumes of no information.

The camera movement in our model is constrained to the trajectory of the mobile mapping system. Therefore it is easy to assume, that these blind spots would not show up in the visualization. But in contrast to the real world objects the visualized ones are flattened. As figure 8 points out, this assumption doesn't hold in the parallax scrolling visualization.

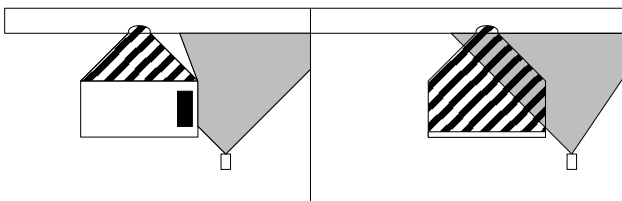


Figure 8: Left: The car is blocking the camera from seeing the blind spot on the wall. Right: The lack of depth on the car enables the camera to see the blind spot.

In order to rectify this problem by making the blind spots invisible again, the positions of the occluding objects have to be altered. The first step is finding the corresponding occluders for the holes. This is done by first finding the holes in the textures of the objects, which are not in the topmost layer. For this we determine the connected components of the texture in regards to pixels, which are marked as holes, using a two-pass algorithm as described by (Azriel Rosenfeld, 1966). Then we calculate the bounding boxes of these connected components and transform them from texture space to model space. The corresponding occluder for a hole is now the closest object that lies completely in front of the bounding box. Now that we know the holes for each occluding object, we can adjust the position, such that the holes will not be visible in the visualization. For this we show two variants in this paper:

1. Static hiding
2. Movable hiding

5.1 Static Hiding

The basic idea is, that the hole is not visible, if its occluding object moves at the same speed (they do not move relative to each other, hence naming it "static"). In order to achieve this, the object needs to be pushed back, so that it is just in front of the hole,

as shown in figure 9. It must not be put in the same layer as the hole to avoid confusion in the drawing order. If the object corresponds to more than one hole, the one nearest to the camera is chosen, otherwise the object would be placed behind a hole, which makes hiding it impossible.

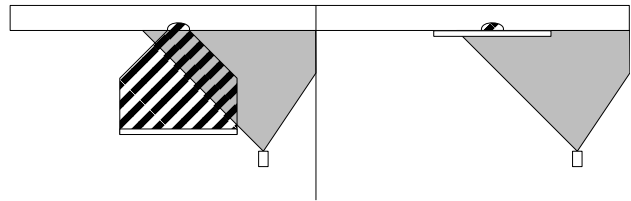


Figure 9: Left: The original scene. Right: The scene with the use of static hiding.

While this variant does fulfill its task of hiding the blind spots, it performs radical changes to the scene. Often foreground objects are pushed noticeably far back, being practically wallpapered onto another object.

5.2 Movable Hiding

Static hiding often pushes objects too far back. In the original scene those objects are not pushed back far enough. From these observations we can conclude, that there must be an optimal distance, at which the occluder is just near enough to the hole to hide it, but can still move relative to it. Finding and relocating the occluding object to this distance is the task of movable hiding.

In order to determine that distance we first assume, that the hole lies centered behind the occluding object, which is depicted in figure 10. In that figure the camera is placed in two positions, such that the hole is just outside of the camera image. The goal is to calculate the distance d , which determines how far in front of the hole the occluder must be placed.

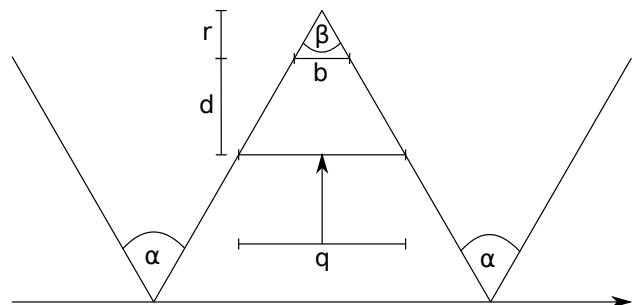


Figure 10: Birds-eye view on the movable hiding situation.

Let α be the aperture of the camera, b the width of the hole and q the width of the occluder. The edges of the two camera cones meet behind the hole and form a triangle with the hole, one with the desired position of the occluder and one with the camera movement line. It is obvious, that the angle β at that point is equal to α . With α and b we can calculate the distance r between the triangle point and the hole.

$$r = \frac{b}{2} \cdot \cot\left(\frac{\alpha}{2}\right) \quad (5)$$

We can also calculate the distance $r + d$ to the desired position of the occluder.

$$r + d = \frac{q}{2} \cdot \cot\left(\frac{\alpha}{2}\right) \quad (6)$$

Now we can determine d through simple subtraction.

$$d = \frac{q}{2} \cdot \cot\left(\frac{\alpha}{2}\right) - \frac{b}{2} \cdot \cot\left(\frac{\alpha}{2}\right) = \frac{q-b}{2} \cdot \cot\left(\frac{\alpha}{2}\right) \quad (7)$$

The distance to the camera of the occluder can now simply be set to the distance to the camera of the hole minus d .

If the hole is not centered behind the occluder, we can artificially enlarge the hole to one side until the state is fabricated. Also, if the occluder corresponds to more than one hole, we calculate the new distances to the camera for every hole and take the biggest distance. If that distance is further away than the nearest hole, we use static hiding instead.

5.3 Hole-Filling

Another fact decreasing the visualization quality are holes that are not caused by occlusion. Empty areas that are not occluded are usually caused by materials that do not reflect the laser beams. Glass is such an material, so windows often result in rectangular holes in the facades texture images as depicted by figure 11.



Figure 11: Building facade containing holes caused by windows.

Detecting and classifying those holes/windows within the image data is a bit out of scope of this paper and is already addressed by various other publications like (Ali et al., 2007). As mentioned earlier, our approach uses a connected component analysis in order to find the corresponding holes. The actual filling will be discussed in the following in more detail. The algorithm distinguishes between two types of holes, small and big ones.

Small holes are probably not caused by windows rather by another material not reflecting the laser beam. That's why small holes are filled by interpolation. As the first step the colored border pixels of the hole are determined. Based on the location and color of those pixels two dimensional function is approximated for each color channel. In the end a color for all pixels is derived based in the determined functions, while the pixel coordinates are used as input values.

Big rectangular holes, in contrast to small holes, are very likely caused by windows. Since the border of those holes are represented by the corresponding window frames, interpolating the color between those is not a good idea, because the frame's color usually has nothing to do with the color of the window's glass. Therefore those holes are covered by a gray rectangle mimicking the window's glass. For a more natural visualization some noise is added as well. The result is shown in figure 12. While the three small holes in the upper part are filled using the approximated color functions, the big holes are covered by gray rectangles.



Figure 12: Building facade with filled holes.

6. IMPLEMENTATION AND RESULTS

The implementation of the visualization was done in Java, using the "Lightweight Java Game Library" (Lightweight Java Game Library, 2013) for its OpenGL bindings. While the usage of a 3D-capable graphics library is in no way necessary, as indeed no 3D-functions of OpenGL were used, we used it for its efficient handling and rendering of textured faces.

The first step when loading the scene is to prepare it for efficient rendering. This consists of translating the scene such that the camera starts of in the middle of it, scaling the layers by their distances and calculating their speeds. The translation is done by calculating the scenes 2D-bounding box (ignoring the depth), determining the position of its middle and translating every layer, which means every quad in a layer, such that the new middle position of the bounding box is at $\begin{pmatrix} 0 \\ 0 \end{pmatrix}$. Scaling and speed calculation are done as described in chapter 3.

After that, the quads of every layer, as well as their textures, are uploaded into OpenGL memory. Each quad consists of four vertices, which consist of their two dimensional spacial positions, as well as their two dimensional texture coordinates. Because OpenGL has a limitation on the maximum size of a texture, we can not just combine every quad of a layer into one big quad.

The rendering of the scene is done as described in chapter 3. At first we clear the screen. Then the stack of layers is rendered bottom to top. Each layer is rendered by rendering all its contained quads, which are stored as vertex buffer objects and references to their textures. The translation of each layer with regards to the simulated camera position is done in the vertex shader and works as in equation (4), with a few exceptions. The vertex positions are already scaled according to their layers distance. Also, OpenGLs screen coordinates are always $\in [-1, 1]$ for both dimensions, no matter if the screen is actually square or not. Therefore it is necessary, to add the aspect ratio as a factor for the y-coordinate. The fragment shader just does a texture lookup.

6.1 Results

The different scaling and speeds of the layers does create an illusion of depth, when the camera is moved. But we had to restrict the camera movement in y-direction to a small interval. The camera should not be able to move down below street level, as that gives the impression that the objects were flying. The camera should also not be able to move too far up, as the lack of depth on an object (especially the lack of a roof) gives the impression that there are huge gaps between objects. The resulting visualization is shown in figure 13. Since the depth illusion results from the different moving layers during an animation, the shown figure hardly does justice to the scheme.

Moreover, the figure also reveals various problems not necessarily related to the proposed visualization scheme. For instance, some building parts mainly in the upper region are missing. This is caused by the fact that the acquisition vehicle was passing too closely by the corresponding building, which means the cameras taking the pictures used for coloring the point-cloud were also very close. The closer the camera is the less of the buildings facade is covered by the resulting image, which results in missing colors for the corresponding points. Furthermore, the shown tree in the center shows also weird colors. This results from the fact that the used camera might not have been calibrated correctly and the tree points are mapped to pixels in between the tree branches. This are basically pixels from the sky and therefore often blue or white.



Figure 13: Resulting parallax scrolling visualization.

One motivation for the proposed visualization scheme was the inability of modern hardware to render massive mobile mapping point-clouds in real-time. The rendering of a single frame took less than a millisecond for the implemented prototype on a modern computer, which allows a theoretic framerate of 1000 fps, enabling even low-end devices or web-based applications.

7. CONCLUSIONS AND FUTURE WORK

This work introduced a new visualization scheme for massive mobile mapping data based on the parallax scrolling technique. An overview of layered models are derived from the mobile mapping point-cloud data, especially the identification of relevant layers is discussed. As shown in chapter 5. the presented approach enables interesting ways of dealing with holes caused by occlusion, by recreating the original occlusion situation in the visualized scene. This hiding instead of interpolating bypasses many problems caused by interpolation. Finally an OpenGL-based prototype implementing the proposed scheme was realized. Even with a minimum number of two layers the illusion of depth was clearly perceptible, while amplified by the use of more layers. As the results indicate a real-time rendering of even big datasets is rather unproblematic, and therefore applicable for many scenarios, including even web-based visualizations.

Alongside the actual visualization many issues have to be addressed in later research. In order to enhance the visualization quality the coloring of the original point-cloud has to be improved, e.g. applying a fine-tuned mobile mapping camera calibration as presented in (Hofmann et al., 2014). Moreover more sophisticated layered model building techniques will be evaluated. Another approach to enhance the depth illusion beside the parallax effect is the use of bump or displacement mapping, which could be integrated into future prototypes. While the discussed static and movable hiding schemes present rather basic concepts, more sophisticated approaches are possible, which will also be elaborated in future research.

REFERENCES

Ali, H., Seifert, C., Jindal, N., Paletta, L. and Paar, G., 2007. Window detection in facades. In: *Image Analysis and Processing, 2007. ICIAP 2007. 14th International Conference on, IEEE*, pp. 837–842.

Azriel Rosenfeld, J. L. P., 1966. Sequential operations in digital picture processing.

Efros, A. and Leung, T., 1999. Texture synthesis by non-parametric sampling. In: *Computer Vision, 1999. The Proceedings of the Seventh IEEE International Conference on, Vol. 2*, pp. 1033–1038 vol.2.

Eggert, D. and Sester, M., 2013. Multi-layer visualization of mobile mapping data. *ISPRS Annals of Photogrammetry, Remote Sensing and Spatial Information Sciences*.

Fischler, M. A. and Bolles, R. C., 1981. Random sample consensus: A paradigm for model fitting with applications to image analysis and automated cartography. *Commun. ACM* 24(6), pp. 381–395.

Gobetti, E. and Marton, F., 2004. Layered point clouds: a simple and efficient multiresolution structure for distributing and rendering gigantic point-sampled models. *Computers & Graphics* 28(6), pp. 815–826.

Hofmann, S., Eggert, D. and Brenner, C., 2014. Skyline matching based camera orientation from images and mobile mapping point clouds. *ISPRS Annals of Photogrammetry, Remote Sensing and Spatial Information Sciences II-5*, pp. 181–188.

Jeschke, S., Wimmer, M. and Purgathofer, W., 2005. Image-based representations for accelerated rendering of complex scenes. In: Y. Chrysanthou and M. Magnor (eds), *EUROGRAPHICS 2005 State of the Art Reports, EUROGRAPHICS, The Eurographics Association and The Image Synthesis Group*, pp. 1–20.

Kopf, J., Chen, B., Szeliski, R. and Cohen, M., 2010. Street slide: Browsing street level imagery. *ACM Transactions on Graphics (Proceedings of SIGGRAPH 2010)* 29(4), pp. 96:1 – 96:8.

Lightweight Java Game Library, 2013. <http://www.lwjgl.org/index.php>.

Richter, R. and Döllner, J., 2010. Out-of-core real-time visualization of massive 3d point clouds. In: *7th International Conference on Virtual Reality, Computer Graphics, Visualisation and Interaction in Africa*, pp. 121 – 128.

Vincent, L., 2007. Taking online maps down to street level. *Computer* 40(12), pp. 118–120.

Wahl, R., Guthe, M. and Klein, R., 2005. Identifying planes in point-clouds for efficient hybrid rendering. In: *The 13th Pacific Conference on Computer Graphics and Applications*, pp. 1–8.

Wang, J. and Oliveira, M. M., 2007. Filling holes on locally smooth surfaces reconstructed from point clouds. *Image Vision Comput.* 25(1), pp. 103–113.

Wimmer, M., Wonka, P. and Sillion, F., 2001. Point-based impostors for real-time visualization. In: S. J. Gortler and K. Myszkowski (eds), *Rendering Techniques 2001 (Proceedings Eurographics Workshop on Rendering)*, Eurographics, Springer-Verlag, pp. 163–176.